Electronic Supplementary Material (ESI)

Hierarchical TiO_2/C nanocomposite monoliths with a robust scaffolding architecture, mesopore-macropore network and TiO_2-C heterostructure for high-performance lithium ion batteries

Hai-Bo Huang,[1]† Yue Yang,[2]† Li-Hua Chen,[*2] Yun Wang,[1] Shao-Zhuan Huang,[2] Jia-Wei Tao,[1] Xiao-Ting Ma,[1] Tawfique Hasan,[3] Yu Li,[2] Yan Xu[* 1] and Bao-Lian Su[*2,4,5]

[1]State Key Lab of Inorganic Synthesis and Preparative Chemistry, Jilin University, Changchun, 130012, China. E-mail: yanxu@jlu.edu.cn

[2]State Key Laboratory of Advanced Technology for Materials Synthesis and Processing, Wuhan University of Technology, 430070, Wuhan, China. E-mail: chenlihua@whut.edu.cn; baoliansu@whut.edu.cn

[3]Cambridge Graphene Centre, University of Cambridge, Cambridge, CB3 0FA, UK.

[4]Laboratory of Inorganic Materials Chemistry, University of Namur, B-5000 Namur, Belgium. E-mail: bao-lian.su@unamur.be

[5]Department of Chemistry and Clare Hall, University of Cambridge, Cambridge, CB2 1EW, UK. E-mail: bls26@cam.ac.uk

† These authors contributed equally to this work

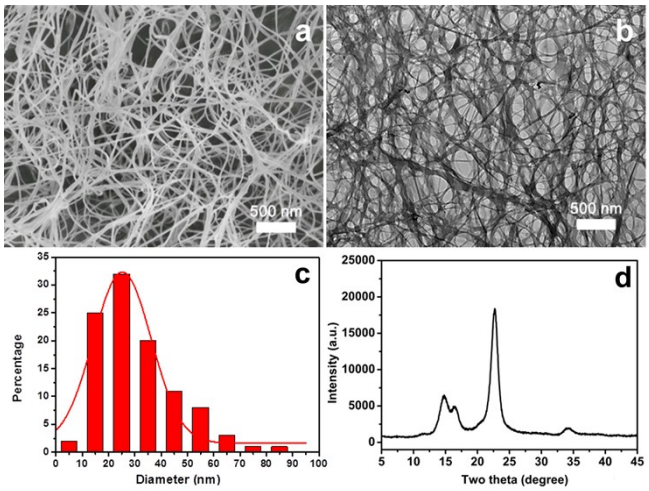

Fig. S1 Characterizing BC aerogel: (a) SEM image. (b) TEM image. (c) Histogram showing the diameter distribution of BC nanofibers. (d) XRD pattern.

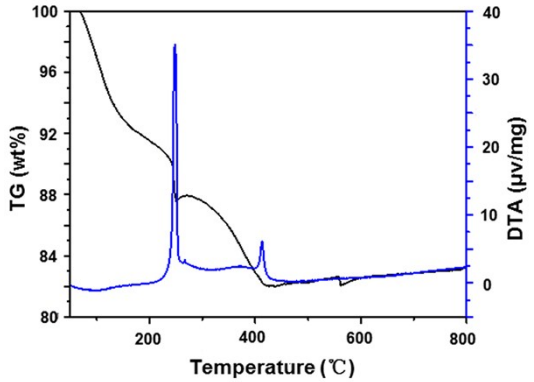

Fig. S2 TG/DTA curves of BC@TiO_2.

Table S1 Average particle size of anatase TiO_2 in TiO_2/C-T

Samples	TiO_2/C-400	TiO_2/C-500	TiO_2/C-600	TiO_2/C-700	TiO_2/C-800	TiO_2-500
Nanoparticle size[a] (nm)	4.2	7.0	12.5	20.7	38.8	9.8

[a]calculated using the Scherrer's equation

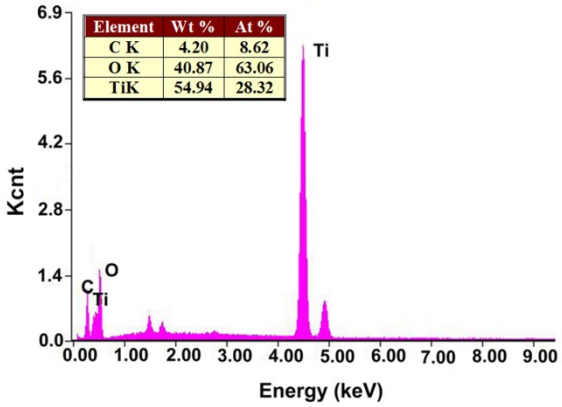

Fig. S3 EDX spectrum of TiO_2/C-500 monoliths.

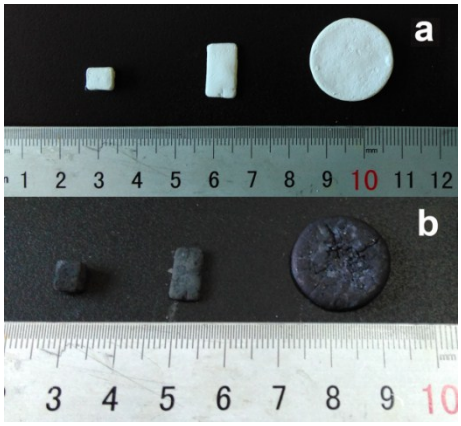

Fig. S4 (a) Photograph of BC@TiO_2 monoliths, (b) Photograph of TiO_2/C-500 monoliths.

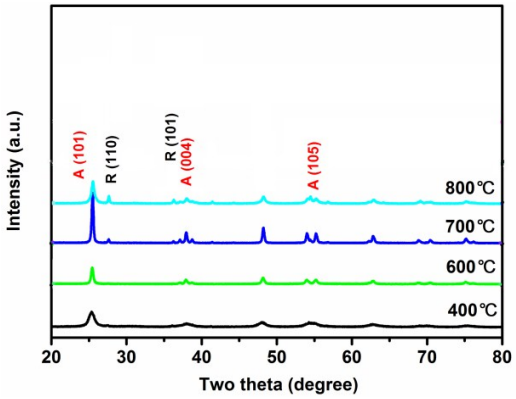

Fig. S5 XRD patterns of TiO_2/C-T monoliths in nitrogen atmosphere at 400 °C, 600 °C, 700 °C and 800 °C.

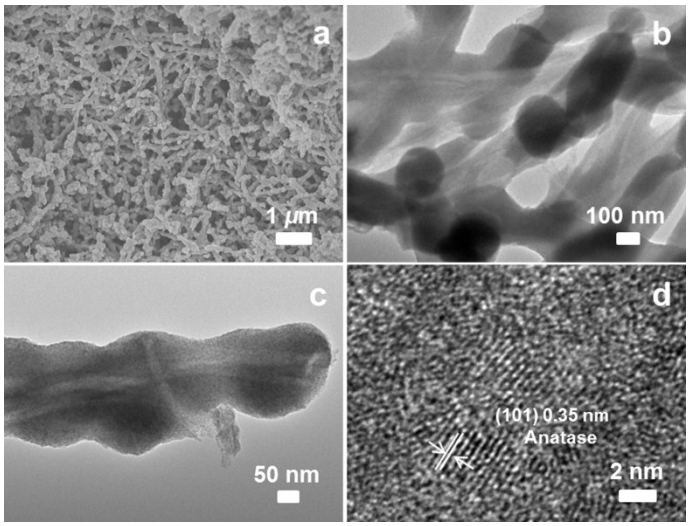

Fig. S6 Characterizing TiO_2/C-400: (a) SEM image. (b) TEM image. (c) High magnification TEM image. (d) HRTEM showing anatase phase.

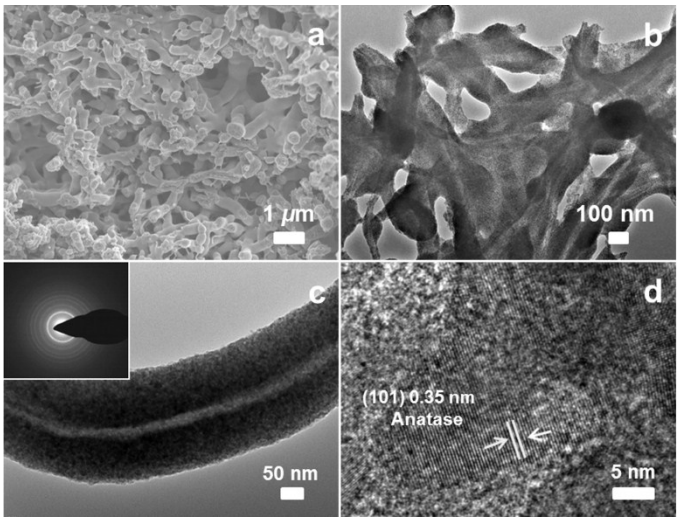

Fig. S7 Characterizing TiO_2/C-600: (a) SEM image. (b) TEM image. (c) High magnification TEM image showing carbon at fiber core. (d) HRTEM showing anatase TiO_2.

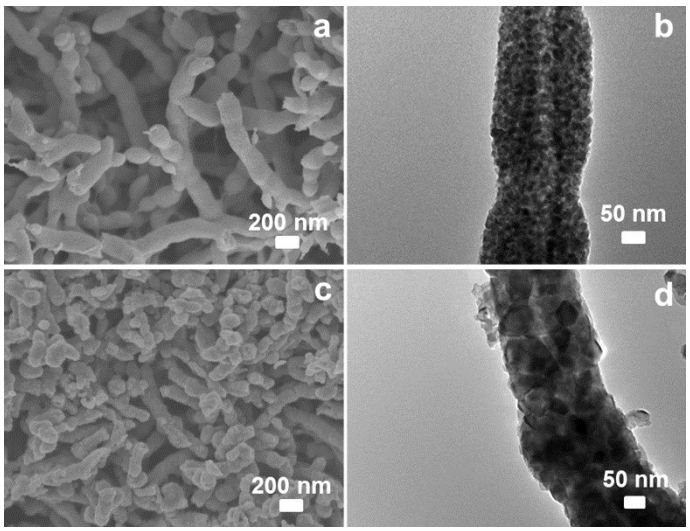

Fig. S8 Characterizing TiO_2/C-700 and TiO_2/C-800: (a) and (b) are the SEM and TEM images of TiO_2/C-700, respectively. (c) and (d) are the SEM and TEM images of TiO_2/C-800, respectively.

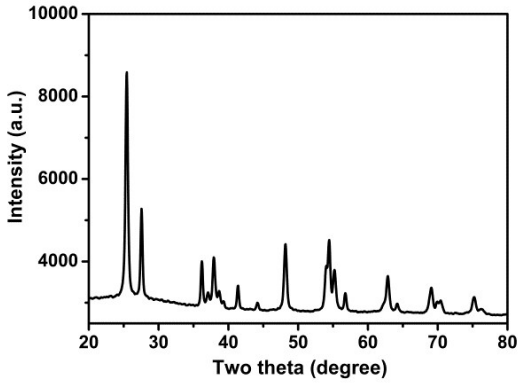

Fig. S9 XRD pattern of TiO_2-500 obtained from the calcination of BC@TiO_2 in air.

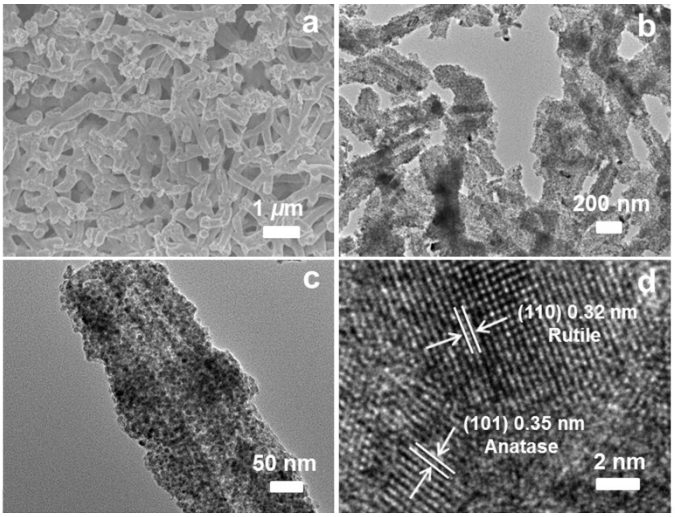

Fig. S10 Characterizing TiO_2-500: (a) SEM image. (b) TEM image. (c) High magnification TEM image. (d) HRTEM showing the presence of anatase and rutile phases.

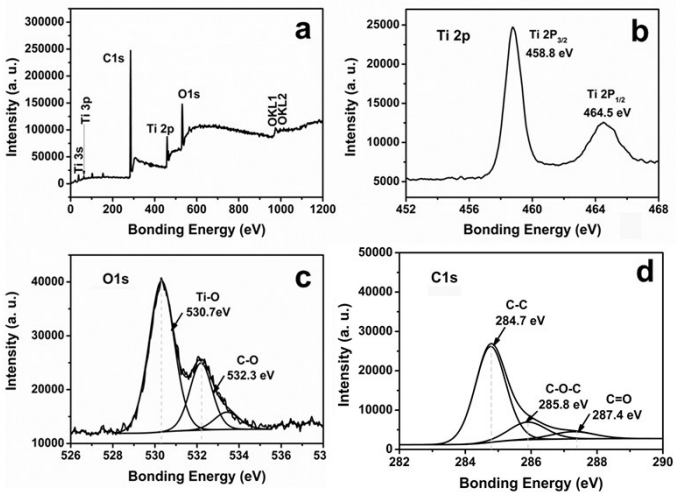

Fig. S11 Characterizing TiO_2/C-500 using XPS: (a) Survey spectrum. The deconvoluted XPS peaks of (b) Ti2p, (c) O1s and (d) C1s.

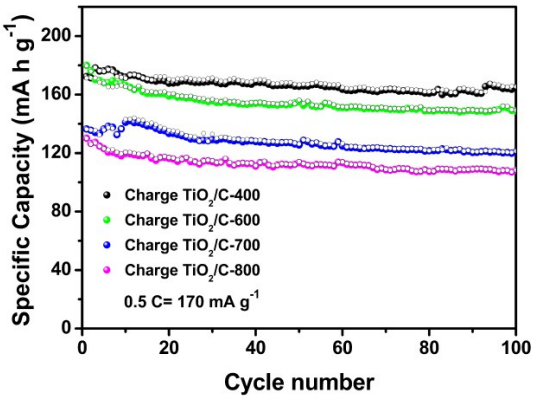

Fig. S12 The cycling performance of TiO_2/C-400, TiO_2/C-600, TiO_2/C-700 and TiO_2/C-800 at 0.5 C.

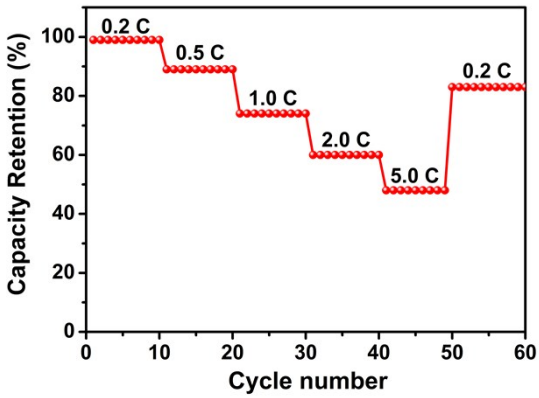

Fig. S13 Capacity retention plots of TiO_2/C-500.

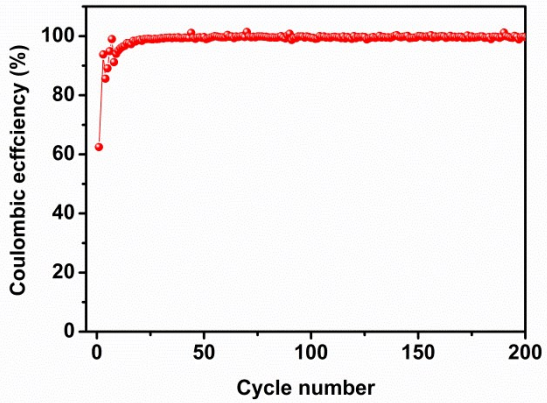

Fig. S14 Coulombic efficiency of TiO_2/C-500 at 0.5 C.

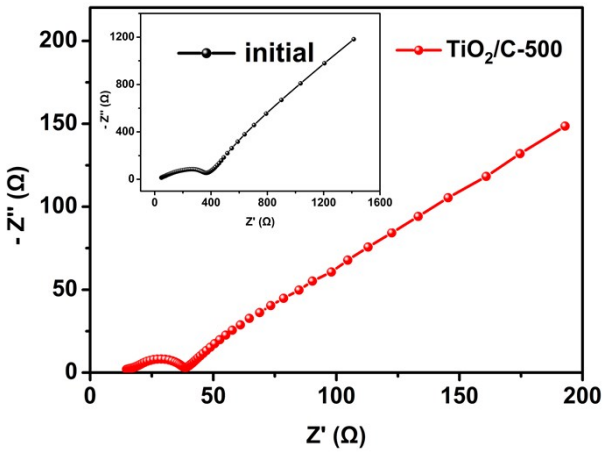

Fig. S15 EIS spectra after 10 cycles and the initial EIS spectra of TiO_2/C-500.

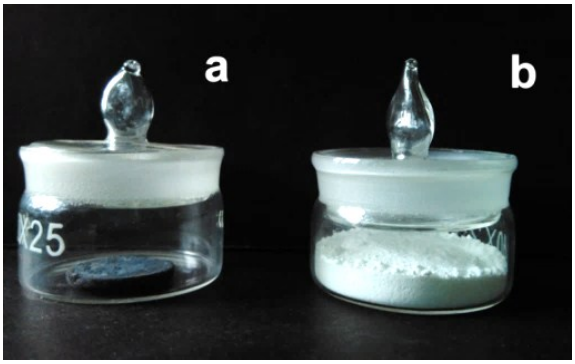

Fig. S16 Comparing the packing density: (a) TiO_2/C-500. (b) P25 nanopowder (0.8 g of each).

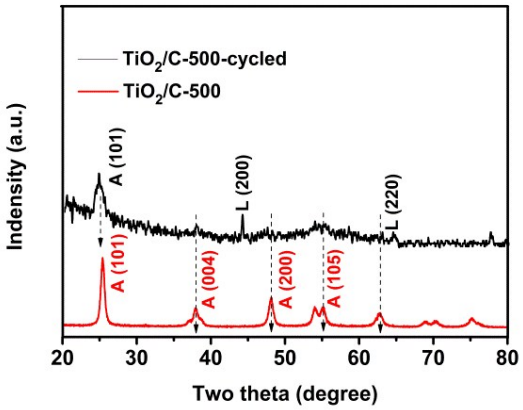

Fig. S17 XRD patterns of TiO_2/C-500 before (red) and after (black) 150 discharge-charge cycles at 0.5 C.